



**Abdualkarim Musbah M. Gariba**  
**Serkan Islak**

Kastamonu University, Kastamonu-Turkey  
abdogareba02@gmail.com; serkan@kastamonu.edu.tr

DOI	<a href="http://dx.doi.org/10.12739/NWSA.2020.15.3.2A0183">http://dx.doi.org/10.12739/NWSA.2020.15.3.2A0183</a>	
ORCID ID	0000-0001-7031-509X	0000-0001-9140-6476
CORRESPONDING AUTHOR	Abdualkarim Musbah M. Gariba	

## CORROSION PROPERTIES OF Ti-B<sub>4</sub>C/CNF FUNCTIONALLY GRADED MATERIALS

### ABSTRACT

This study aims to investigate corrosion properties of Ti-B<sub>4</sub>C/CNF functional graded materials (FGMs). FGMs are produced in three layers by traditional cold pressing and sintering method. While B<sub>4</sub>C was incorporated into the Ti matrix at 5%, 10% and 15% percent, the CNF was only 0.5% by volume. Corrosion properties of FGMs are determined by potentiodynamic method. 3 M HCl was preferred as the corrosion solution. Corrosion rates were calculated from the Tafel curve and the corrosion surface was examined by using SEM-EDS. The results show that the corrosion process of composite material in 3 M HCl showed different corrosion resistance, in which corrosion rate showed the evolution trend of initial increase and subsequent decrease, while amount of reinforcement changed. While the best corrosion resistance among the FGMs was determined in the sample with 5%B<sub>4</sub>C additive, the worst corrosion resistance was determined with 15%B<sub>4</sub>C+0.5% CNF additive.

**Keywords:** FGMs, B<sub>4</sub>C, CNF, Titanium, Corrosion

### 1. INTRODUCTION

Titanium is strong metal with low density of 4.5g/cm<sup>3</sup>. It is located in about halfway between aluminium and steel. Its strength to weight ratio made it an excellent choice for aircraft and ordnance where it was first introduced as a structural material [1, 2 and 3]. For its lightweight and strong properties, titanium is now widely utilized in the space and chemical process industries [4 and 5]. Similar to steels, titanium as a pure element is very strong material, however; its density is a little low. Therefore, this chemical element may be mixed with some other elements for example iron, aluminium, to make it more stronger and less weight composites. This composites can be used in different industrial processes like aircraft industry, military, car production, medical and dental implants [6]. One way of these modifications and making new alloys is by using Functionally graded materials (FGMs). This FGMs have been increasingly used during the recent years for several engineering applications such as airoplane, marine, car manufacturing, and electronic industries [7, 8, 9, 10 and 11]. FGMs is a highly modified engineering material that is able to persist in a severe working conditions, however their properties can last for a longer period of time, and it remains resistant to stop while working. It is categorized by adding gradually some material into another, which become a new material that are either mixtures that have properties in the half way between the added material, or a mixture of two compounds that joined together but with each of them keeps its property. FGMs are ingredients that are made to functionally work in different requirements. B<sub>4</sub>C is considered to be the

#### How to Cite:

Musbah M. Gariba, A. and Islak, S., (2020). Corrosion Properties of Ti-B<sub>4</sub>C/CNF Functionally Graded Materials, Technological Applied Sciences (NWSATAS), 15(3):41-49, DOI:10.12739/NWSA.2020.15.3.2A0183.



third hardest material after diamond and boron nitride, therefore it is highly produced in big quantities. It was firstly discovered in mid 19<sup>th</sup> century as a by-product in the production of metal borides, boron carbide was only studied in detail since 1930 [12]. Another useful property is that it directly synthesizes from carbon and boron elements with the help of metallothermic procedure.

Carbon nanofiber (CNF) is considered to be high and strong material and has good thermal and electrical properties. Therefore; it is used for a range and different applications for example; it is used as catalyst support, electromagnetic wave shielding, electrodes of the cell, and reinforcement construction [13, 14, 15 and 16]. The different physical forms of each of two or more carbon elements can exist, makes several allotropes (graphite, diamond, carbon nanotube, carbon nanofiber, etc.) for the distribution their bonding, therefore carbon can be processed in the forms of powder, fiber, and foam. Since carbon has a large surface area, this feature gives it the possibility to be used in high conductivity, depending on the structure of the graphite, and therefore it has a large use area in energy storage operations.

## **2. RESEARCH SIGNIFICATION**

Titanium is a reactive metal and depends on a protective film for corrosion resistance because it forms an oxide layer on the top of its surface, which as a result gives the material more protection and degreases the oxidation process in the corrosive environments [17, 18, 19, 20 and 21]. However, the presence of FGMs namely; its alloys with presence of different concentration of B<sub>4</sub>C and CNF needs and required more studies and is a good topic for investigation. Therefore; the goal of this research was to investigate the corrosion behavior of different composites of FGMs of Ti, B<sub>4</sub>C and CNF in the corrosive environment of 3 M HCl.

## **3. EXPERIMENTAL STUDIES**

### **3.1. Production of FGMs**

In the present study, the starting materials chosen were titanium powders as matrix (-325 mesh particle size, 99.9% purity), with reinforcement powders of B<sub>4</sub>C (400 mesh particle size, ≥97.5% purity) reinforcement powders of CNF (D×L 100 nm×20-200 μm particle size, >98 purity). Samples were prepared by adding B<sub>4</sub>C particles to Ti powder at different rates of 5%, 10% and 15% by volume. Three more similar samples were prepared by adding CNF at rate of 0.5% by volume. Then, the powders were subjected to mixing for 45 minutes at speed of 20 rpm with 10 steel milling balls (10mm diameter). In cold pressing process, the powder were placed in a mold with a 24×10mm. FGMs for each sample were manufactured in three layers. The outer layers were made of Ti+B<sub>4</sub>C and Ti+B<sub>4</sub>C+CNF composite and the inner layer was made of pure Ti material. The reinforcement powder was added to the powder matrix in upper and lower layers and pressed at 500 MPa by cold pressing to produce a 4.5 mm thick composite sample with a 24×10mm (with three 1.5mm layers) as showing in Figure 1. The samples Ti-matrix composite reinforced by B<sub>4</sub>C and CNF were sintered in a tube furnace under a protective argon gas atmosphere with 1300°C [22] and the duration was 60 minutes with a heating and cooling rate of 10°C/min.



Figure 1. The sample shape

### 3.2. Electrochemical/Corrosion Cell and Equipment

Corrosive solution (electrolyte) was prepared by diluting 25ml of concentrated 37% HCl to final 100 ml by adding 75ml of distilled water. The electrochemical/corrosion cell consisted of three-electrodes that was applied in electrochemical experiments. The graphite was used as a counter electrode. The saturated calomel electrode (SCE) was used as a reference electrode [23]. The working electrode was prepared from FGMs. Corrosion tests consisting in potentiodynamic polarization (PDP) were done in 3 M HCl solution at room temperature after 30 min at open circuit potential (OCP) to equilibrium. The Gamry Potentiostat/Galvanostat (model Reference 3000) was used to perform the Tafel measurement. Corrosion test system used in corrosion tests is shown in Figure 2. The polarization scan was performed of the working electrode ca. -250 mV to 250 mV with a scanning rate of 1 mVs<sup>-1</sup>. Before each experiment, the working electrode surface was grinded with 400, 600, 800 and 1200 silicon carbide grit sand paper, then; the surface was polished with the help of diamond spray to give a mirror like surface finish, and then carefully rinsed with distilled water. After this, the electrode was degreased with ethanol and then dried with hot air. Then the epoxy resin was used to protect the sample leaving an area of 1.4 cm<sup>2</sup> that can be used for solution exposures. All the measurement of current and potential are normalized with respect to the surface area of the electrode.



Figure 2. Corrosion test system

## 4. FINDINGS AND DISCUSSIONS

### 4.1. Tafel Polarization Measurements

The Tafel curves of the Ti, with at different compositions of B<sub>4</sub>C+CNF composites determined in the 3 M HCl corrosive medium, are illustrated in Figure 3. The results of the Tafel measurements are summarized in Table 1. Corrosion potential ( $E_{\text{corr.}}$ ), anodic and cathodic Tafel slopes ( $\beta_a$  and  $\beta_c$ ), corrosion rate and corrosion current ( $i_{\text{corr.}}$ ) were found from Tafel curves. As seen in Figure 2 and Table 1, the corrosion potentials of the composites are quite different from each other which more clearly shown in the anodic Tafel curves. The Tafel curve of the unreinforced pure Ti shows lower corrosion current  $i_{\text{corr.}} = 0.164 \mu\text{Acm}^{-2}$  which in contrast a higher corrosion resistance. It also

has a more positive potential in comparison to the other composites. In comparison to the pure material of Ti, the Tafel curves for the Ti composite is changing at each amount of reinforcement and showed different corrosion resistance behavior in 3 M HCl environment. The corrosion resistance of reinforced composites was lower than the corrosion resistance of unreinforced Ti material. It can be seen from the Table 1 that the corrosion current values increase with the increase of the composites contents in the both case of B<sub>4</sub>C+CNF. The lowest value of 105  $\mu\text{Acm}^{-2}$  was found at the composite at the concentration Ti+5%B<sub>4</sub>C whereas the highest corrosion current of 869  $\mu\text{Acm}^{-2}$  was found at the concentration of Ti+15%B<sub>4</sub>C+0.5%CNF. This is due to differences in electrochemical potential between B<sub>4</sub>C+CNF and Ti. The corrosion rate is presented in Table 1. It seems that very low concentration (Ti+5%B<sub>4</sub>C) of B<sub>4</sub>C leads to a large gradation increase of corrosion performance. This is much clearer from the data shown in Figure 3, as one can deduce an exponentially stabilized behaviour of corrosion rate with extra additions of B<sub>4</sub>C and CNF as shown in sample number 6. This corrosion rate shows quite the same behaviour and it increased proportionally to the corrosion current; i.e. by increase the contents of the B<sub>4</sub>C+CNF contents the corrosion rate also increases. This can be explained as by increasing in grain size in the composites by increase in its concentration, causes the composite material to be more porous. A more porous structure is exposed to more corrosion because chlorine ions can penetrate through these pores and show corrosive effect on composite material.

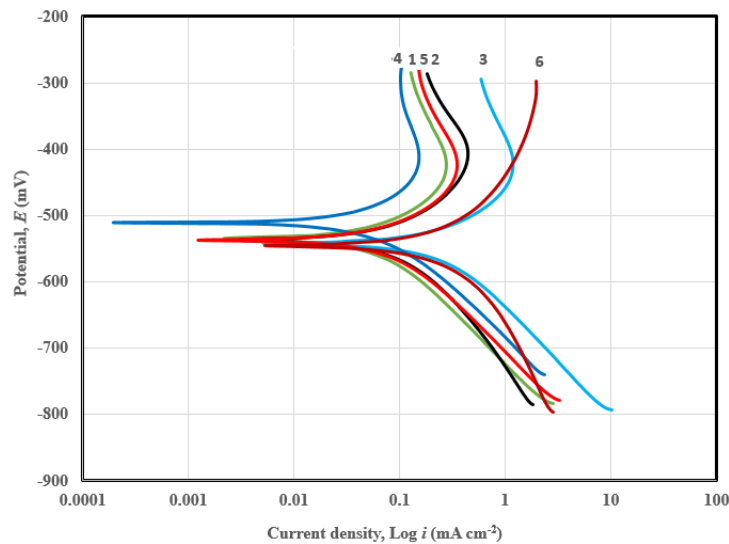


Figure 3. Tafel plots: (1)Ti+5%B<sub>4</sub>C, (2)Ti+10%B<sub>4</sub>C, (3)Ti+15%B<sub>4</sub>C, (4)Ti+5% B<sub>4</sub>C+0.5%CNF, (5)Ti+10%B<sub>4</sub>C+0.5%CNF and (6)Ti+15%B<sub>4</sub>C+0.5%CNF

Table 1. Corrosion potential, corrosion current, Tafel slopes and corrosion rate calculated of Ti-B<sub>4</sub>C+CNF FGMs recorded at 3 M HCl at room temperature

No	Samples	$E_{corr.}$ (mV)	$i_{corr.}$ ( $\mu\text{Acm}^{-2}$ )	$\beta_a$ (mV/decade)	$B_c$ (mV/decade)	Corrosion Rate CR (mpy)
1	Ti+5%B <sub>4</sub> C	-535	105	162.2	225.4	87.4
2	Ti+10%B <sub>4</sub> C	-537	246	274.3	386.9	197.6
3	Ti+15%B <sub>4</sub> C	-542	517	204	285.7	436.5
4	Ti+5%B <sub>4</sub> C+0.5%CNF	-531	152	344.4	506.8	176.2
5	Ti+10%B <sub>4</sub> C+0.5%CNF	-537	187	224.8	308.1	220.5
6	Ti+15%B <sub>4</sub> C+0.5%CNF	-530	869	277.8	317.5	914.2

#### 4.2. Surface Topography Analysis

The Surface topography of the different composites was studied. Figure 4, Figure 5 and Figure 6 show example of the SEM-EDS analysis that were performed before and after corrosion measurement of the samples in 3 M HCl solution. It can be seen that from Figure 4a, which shows the surface topography of Ti+5%B<sub>4</sub>C surface before corrosion. The surface shows only the polishing surface, on the other hand, from Figure 4b, the surface shows a lighter corrosion. Similarly the effect of corrosion and deterioration on the surface is more visible in the other sample of Ti+10%B<sub>4</sub>C as it is shown in Figure 5a and Figure 5b before and after corrosion; respectively. Worst corrosion resistance is more clearly visible in the Figure 6a and Fig. 6b for the sample with 15%B<sub>4</sub>C+0.5%CNF. In this case, the surface are more corroded and the most important reason for this can be the rate of reinforcement and porosity. In addition to that the different of amount of reinforcement affects in the rate of corrosion as shown in Figure 6b. It can be seen that corrosion is more visible for the reason of porosities. Considering all these results, and compared to Table 1, it is determined that the best corrosion resistance is in first sample with 5% B<sub>4</sub>C and the worst corrosion resistance is in sixth sample with 15%B<sub>4</sub>C+0.5%CNF. The most important reason for this can be the rate of reinforcement and porosity.

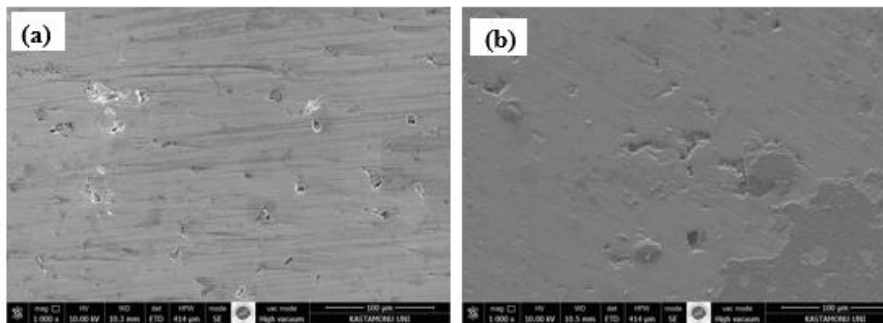


Figure 4. SEM images of Ti+5%B<sub>4</sub>C sample (a) before and (b) after corrosion

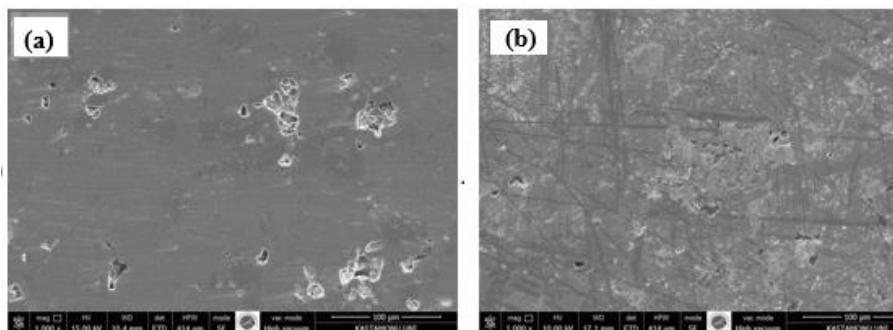


Figure 5. SEM image of Ti+5%B<sub>4</sub>C sample (a) before and (b) after corrosion

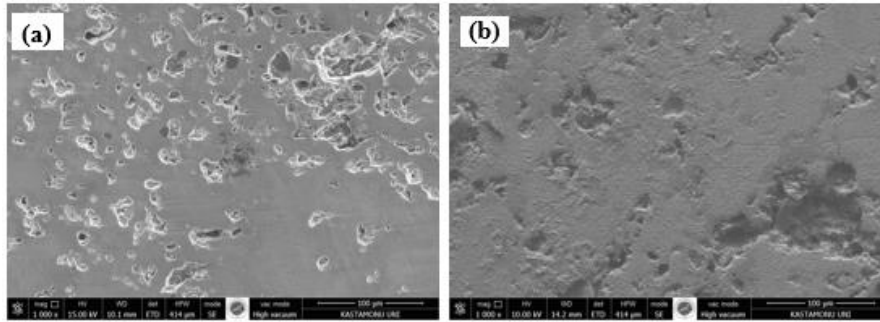


Figure 6. SEM image of Ti+15%B<sub>4</sub>C+0.5CNF sample (a) before and (b) after corrosion

EDS analyses for some selected composites are shown in Figures 7-9. In comparison to the samples before corrosion, it was found that, at the samples after corrosion, the weight rate and atomic rate of the elements is changed. For example, in Figure 7, 3.68% by weight of boron in the case of the sample before corrosion; however; after corrosion, this weight percent become 1.4%, which indicates the decrease of its content because of corrosion. This can be also observed by the appearance of chlorine element that comes from the corrosive solution of HCl, which cause more deterioration of the surface.

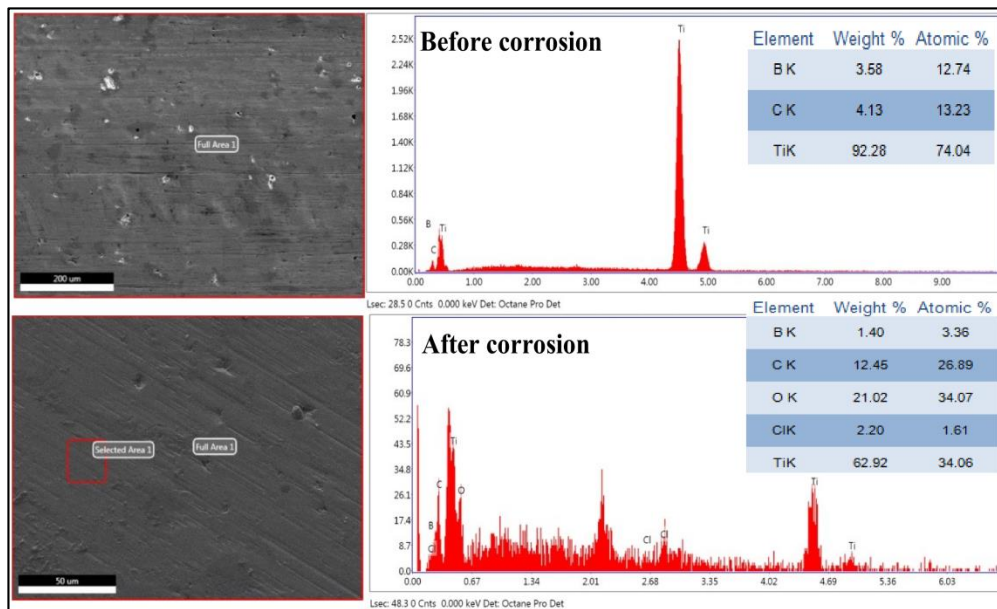


Figure 7. EDS analysis of Ti+5%B<sub>4</sub>C sample before and after corrosion

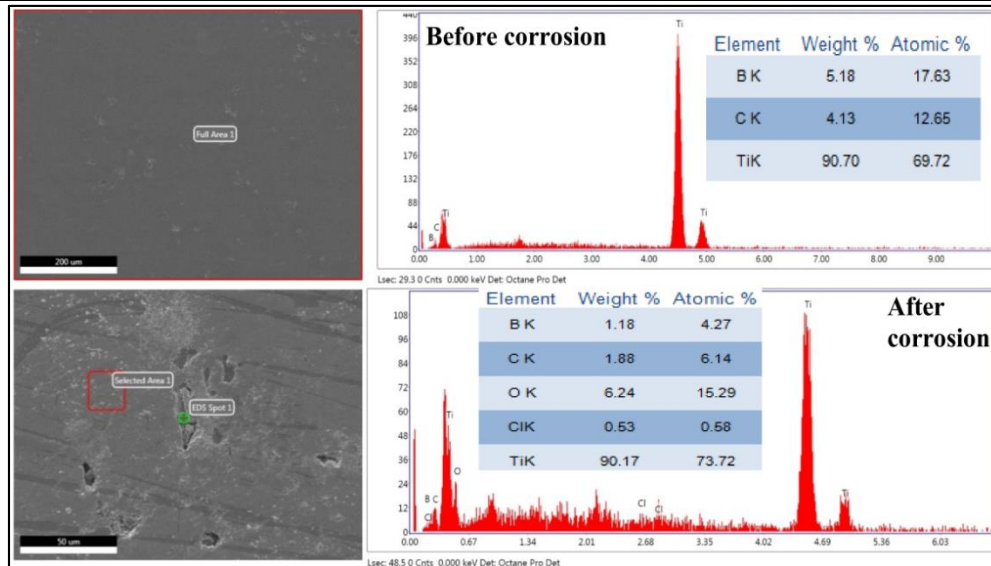


Figure 8. EDS analysis of Ti+5%B<sub>4</sub>C sample before and after corrosion

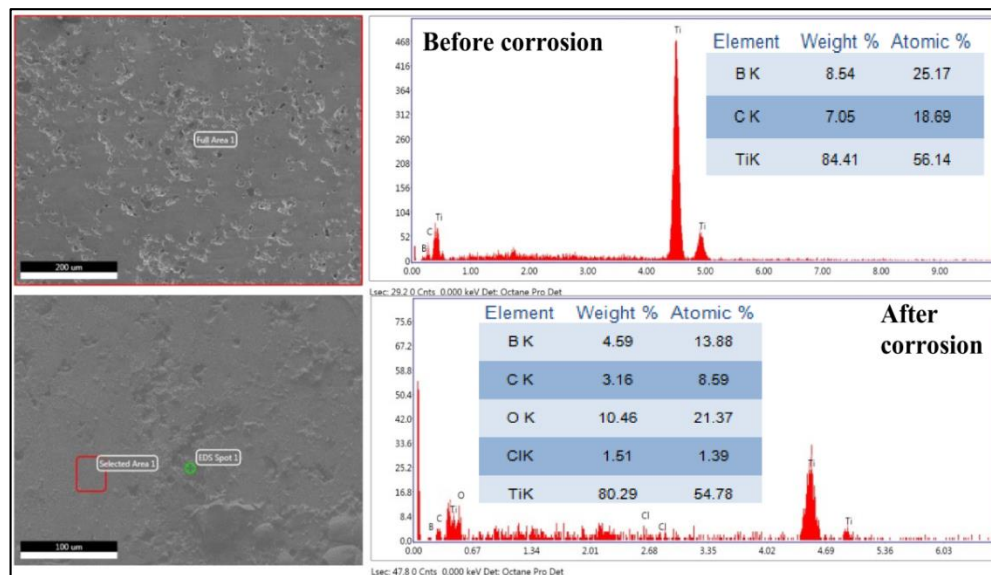


Figure 9. EDS analysis of Ti+15%B<sub>4</sub>C+0.5%CNF sample before and after corrosion

### 5. GENERAL RESULTS

The following main conclusions can be drawn from the present study:

- FGMs were successfully produced by cold pressing+sintering method with Ti powders, B<sub>4</sub>C and CNF particles.
- Corrosion potential ( $E_{corr}$ ), anodic and cathodic Tafel slopes ( $\beta_a$  and  $\beta_c$ ), corrosion rate (CR) and corrosion current ( $i_{corr}$ ) were found from Tafel curves.
- Tafel polarization and scanning electron microscopy were used to evaluate the corrosion behavior of Ti and different compositions of B<sub>4</sub>C+CNF.
- Tafel measurements revealed that the lower corrosion current and also the lower corrosion rate was found in the case of 5%B<sub>4</sub>C composites and it increases by increasing the concentration of the B<sub>4</sub>C+CNF in the composites.



- SEM-EDS analysis show that the surface become more porous structure as the concentration of the B<sub>4</sub>C+CNF increases when is exposed to more corrosion. This gives the chlorine ions to be able to penetrate through these pores and cause more corrosion.

#### REFERENCES

- [1] Ilogebe, A.B., (2016). Development, Liquid Metal Infiltration and Characterization of Binder-Jet Printed Structural Amorphous Metal Alloy (Doctoral dissertation, North Carolina Agricultural and Technical State University).
- [2] Pawelec, K.M., White, A.A., and Best, S.M., (2018). University of Michigan, Ann Arbor, MI, United States; Lawrence Berkeley National Laboratory, Berkeley, CA, United States; University of Cambridge, Cambridge Centre for Medical Materials, Cambridge, United Kingdom. Bone Repair Biomaterials: Regeneration and Clinical Applications, 65.
- [3] Chung, D.D., (2010). Thermal Properties. *Composite Materials: Science and Applications*. 277-331.
- [4] Inagaki, I., Takechi, T., Shirai, Y., and Ariyasu, N., (2014). Application and Features of Titanium for the Aerospace Industry. *Nippon Steel and Sumitomo Metal Technical Report*. 106(106):22-27.
- [5] Lan, Y., Lu, Y., and Ren, Z., (2013). Mini Review on Photocatalysis of Titanium Dioxide Nanoparticles and Their Solar Applications. *Nano Energy*. 2(5):1031-1045.
- [6] Masubuchi, K., (2013). Analysis of Welded Structures: Residual Stresses, Distortion, and Their Consequences (Vol:33). Elsevier.
- [7] Gupta, A. and Talha, M., (2015). Recent Development in Modeling and Analysis of Functionally Graded Materials and Structures. *Progress in Aerospace Sciences*. 79:1-14.
- [8] CPM, S.A., Varghese, B., and Baby, A., (2014). A Review on Functionally Graded Materials. *Int. J. Eng. Sci.* 3:90-101.
- [9] Nikbakht, S., Kamarian, S., and Shakeri, M., (2019). A Review on Optimization of Composite Structures Part II: Functionally Graded Materials. *Composite Structures*. 214:83-102.
- [10] Besisa, D.H. and Ewais, E.M., (2016). Advances in Functionally Graded Ceramics—Processing, Sintering Properties and Applications. *Advances in Functionally Graded Materials and Structures*, 1-32.
- [11] Rathee, S., Maheshwari, S., Siddiquee, A.N., and Srivastava, M., (2018). A Review of Recent Progress in Solid State Fabrication Of Composites and Functionally Graded Systems Via Friction Stir Processing. *Critical Reviews in Solid State and Materials Sciences*. 43(4):334-366.
- [12] Besisa, D.H. and Ewais, E.M., (2016). Advances in Functionally Graded Ceramics—Processing, Sintering Properties and Applications. *Advances in Functionally Graded Materials and Structures*, 1-32.
- [13] Shirvanimoghaddam, K., Hamim, S.U., Akbari, M.K., Fakhrhoseini, S.M., Khayyam, H., Pakseresht, A.H., ... and Davim, J.P., (2017). Carbon Fiber Reinforced Metal Matrix Composites: Fabrication Processes and Properties. *Composites Part A: Applied Science and Manufacturing*. 92:70-96.
- [14] Miranda, A., Barekar, N., and McKay, B.J., (2019). MWCNTs and Their Use in Al-MMCs for Ultra-high Thermal Conductivity Applications: A Review. *Journal of Alloys and Compounds*. 774:820-840.
- [15] Tan, Y.Q., Chen, C., Li, F.Z., Zhang, H.B., Zhang, G.J., and Peng, S.M., (2015). Enhancement of Sinterability and Mechanical



- 
- Properties of B<sub>4</sub>C Ceramics Using Ti<sub>3</sub>AlC<sub>2</sub> as a Sintering Aid. *Rsc Advances*. 5(93):76309-76314.
- [16] Liew, P.J., Nurlishafiqa, Z., Ahsan, Q., Zhou, T., and Yan, J., (2018). Experimental Investigation of RB-SiC using Cu-CNF Composite Electrodes in Electrical Discharge Machining. *The International Journal of Advanced Manufacturing Technology*. 98(9-12):3019-3028.
- [17] Özcan, M. and Hämmerle, C., (2012). Titanium as a Reconstruction and Implant Material in Dentistry: Advantages and Pitfalls. *Materials*. 5(9):1528-1545.
- [18] Bhola, R., Bhola, S.M., Mishra, B., and Olson, D.L., (2011). Corrosion in Titanium Dental Implants/Prostheses—a Review. *Trends Biomater Artif Organs*. 25(1):34-46.
- [19] De Viteri, V.S. and Fuentes, E., (2013). Titanium and Titanium Alloys as Biomaterials. *Tribology-fundamentals and Advancements*. 155-181.
- [20] Thomas, S., Birbilis, N., Venkatraman, M.S., and Cole, I.S., (2013). Self-repairing Oxides to Protect Zinc: Review, Discussion and Prospects. *Corrosion Science*. 69:11-22.
- [21] Chatterjee, U.K., Bose, S.K., and Roy, S.K., (2001). *Environmental Degradation of Metals: Corrosion Technology series/14*. CRC Press.
- [22] Singh, H., Hayat, M., He, Z., Peterson, V K., Das, R., and Cao, P., (2019). In Situ Neutron Diffraction Observations of Ti-TiB Composites. *Composites Part A: Applied Science and Manufacturing*. 124:105501.
- [23] Ghareba, S. and Omanovic, S., (2011). The Effect of Electrolyte Flow on the Performance of 12-aminododecanoic Acid as a Carbon Steel Corrosion Inhibitor in CO<sub>2</sub>-saturated Hydrochloric Acid. *Corrosion Science*. 53(11):3805-3812.